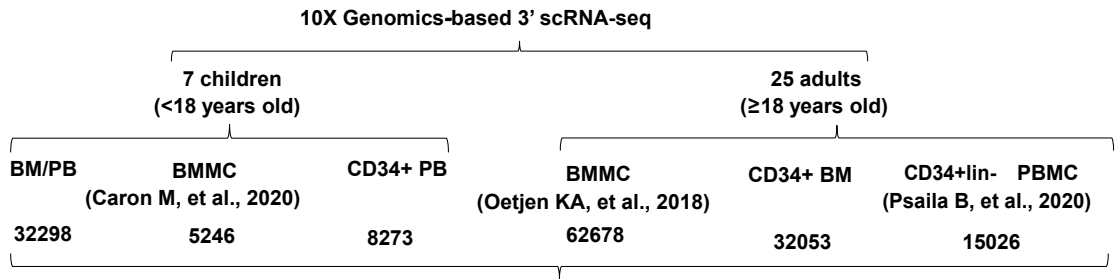


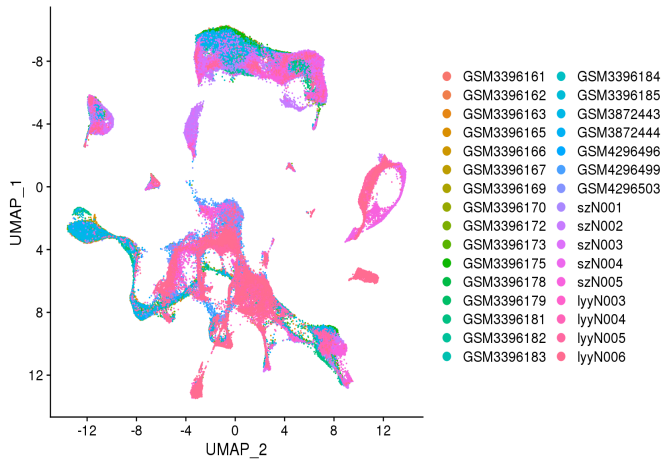
Figure S1

a

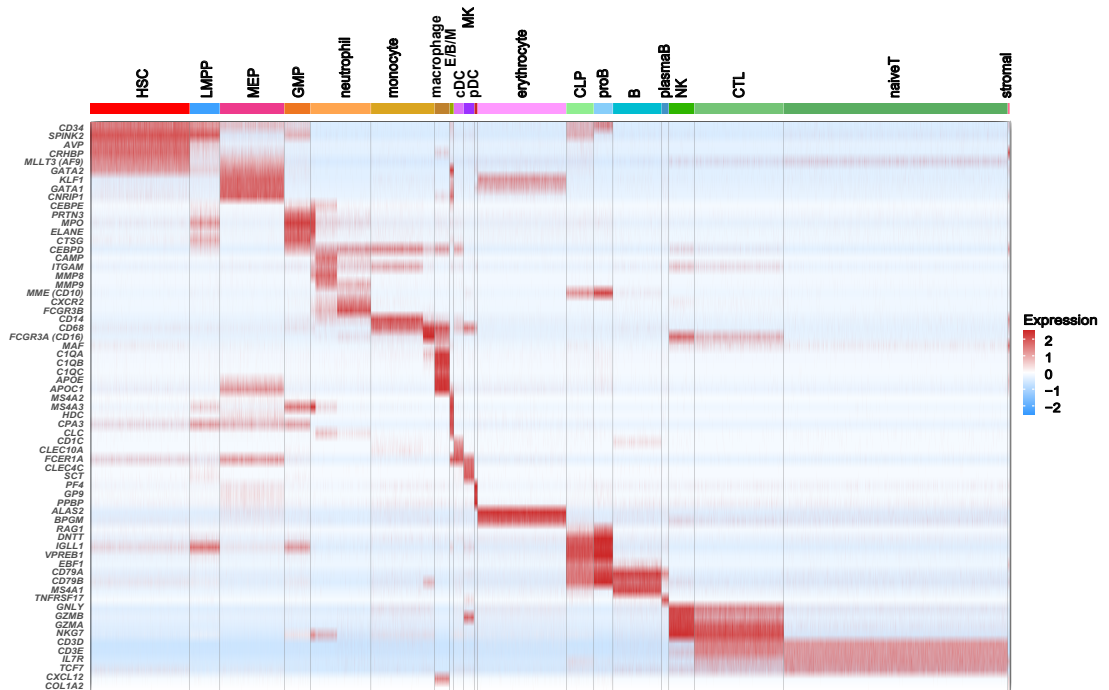


155,574 high quality transcriptomes to establish baseline hematopoiesis landscape

b

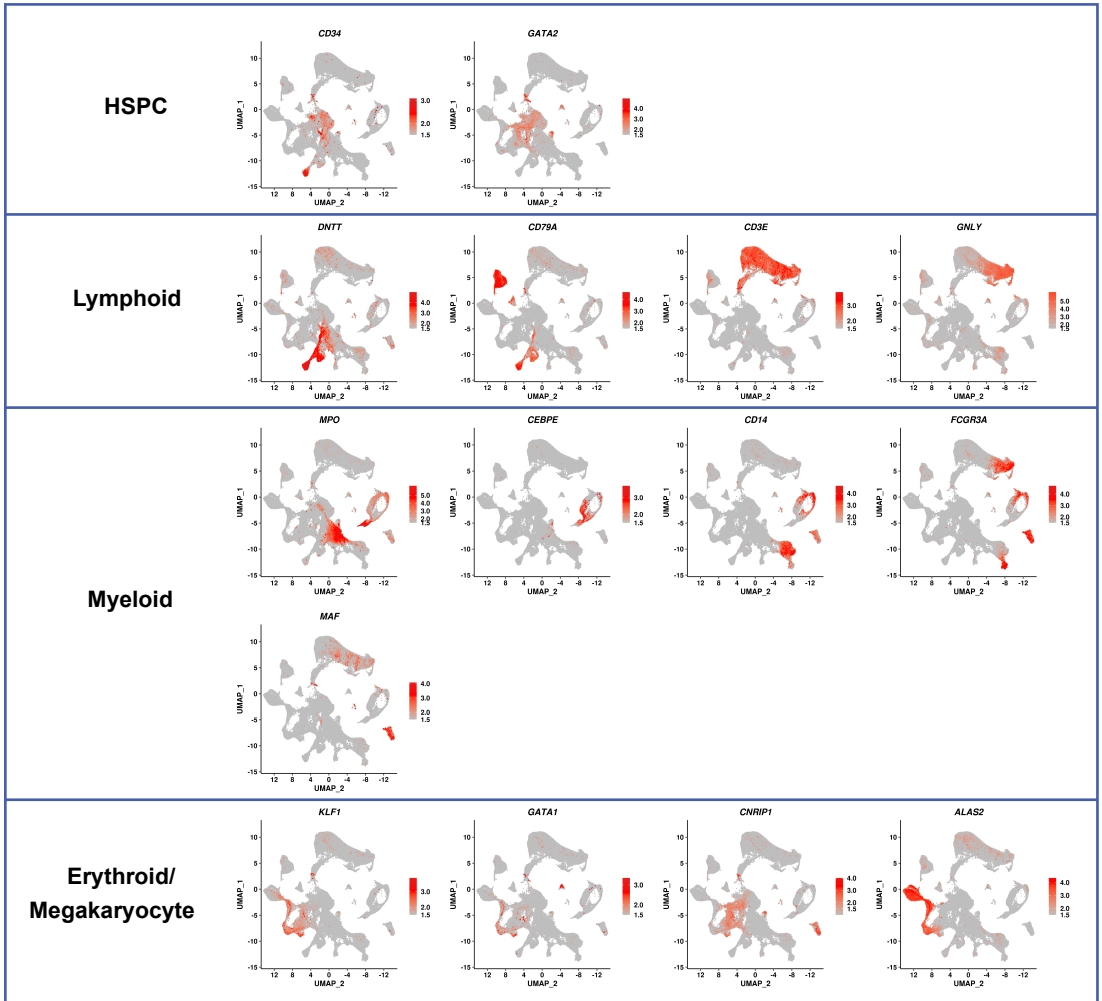


c



continued on next page

d



e

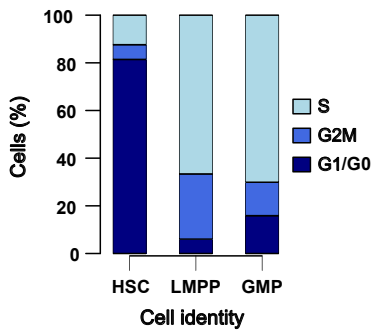


Figure S1. Single-cell profiling of normal hematopoietic cells from healthy donors

a Integration of scRNA-seq data from bone marrow (BM) and peripheral blood (PB) aspirates of healthy donors, including our samples and those from published studies. The numbers below each dataset represent high-quality single cells, and the numbers of pediatric and adult donors are indicated. BMMC: bone marrow mononuclear cell. PBMC: peripheral blood mononuclear cell.

b UMAP visualization of healthy donor data, with cells colored according to sample origins.

c Heatmap showing the relative expression of selected cell type-specific marker genes (rows) across all single cells, ordered by cell types (columns).

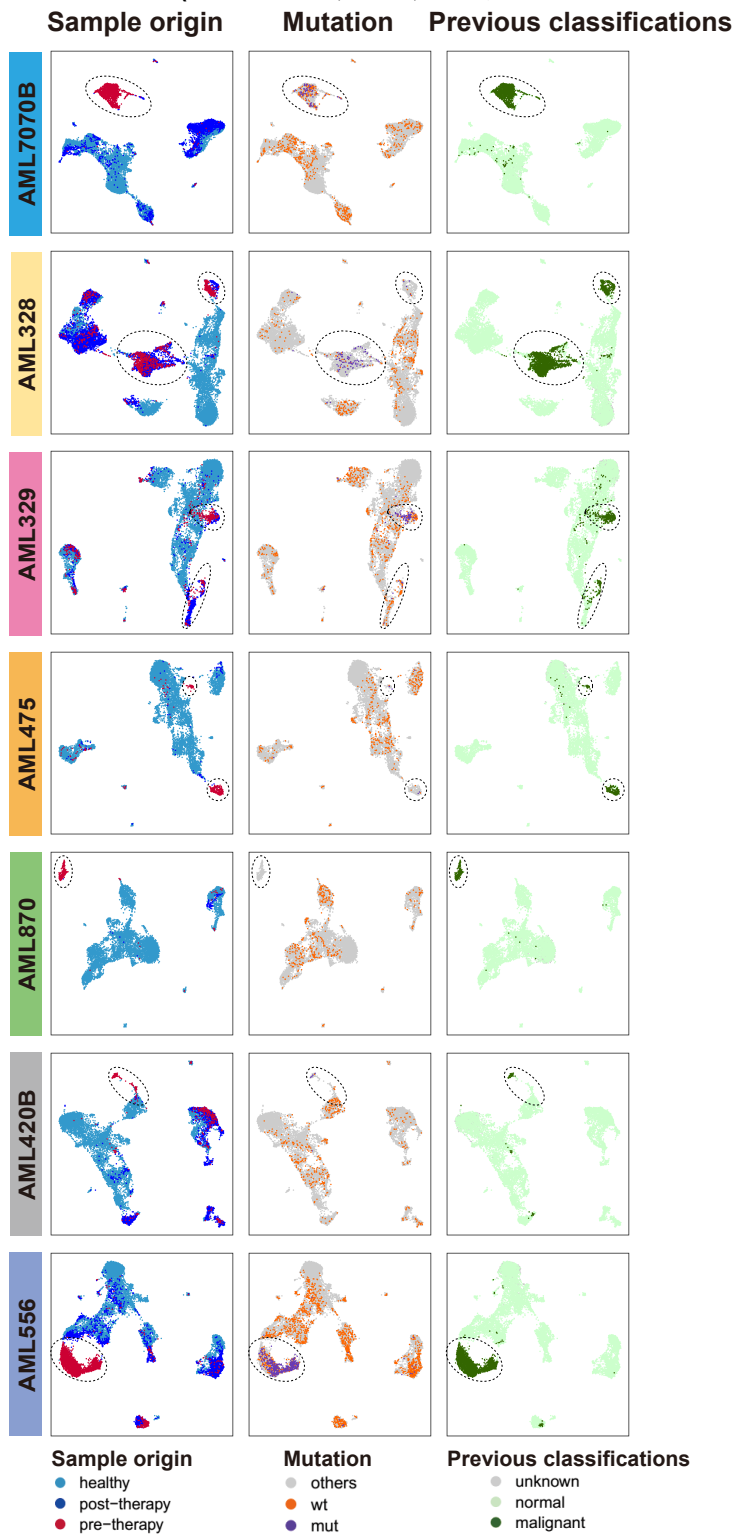
d Feature plots depicting the expression levels of representative known genes specific to hematopoietic stem/progenitor cells (HSPCs), as well as myeloid, erythroid, and lymphoid lineages in all single cells. Each dot represents a cell, and the shading denotes the relative expression level.

e Bar plot representing the frequency of cell cycle phases in HSPCs.

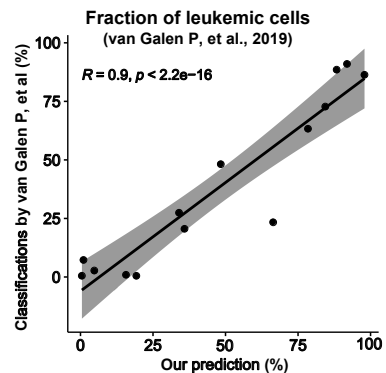
Figure S2

a

(van Galen P, et al., 2019)



b



Continued on next page

C**transcriptionally
predicted malignant cell**

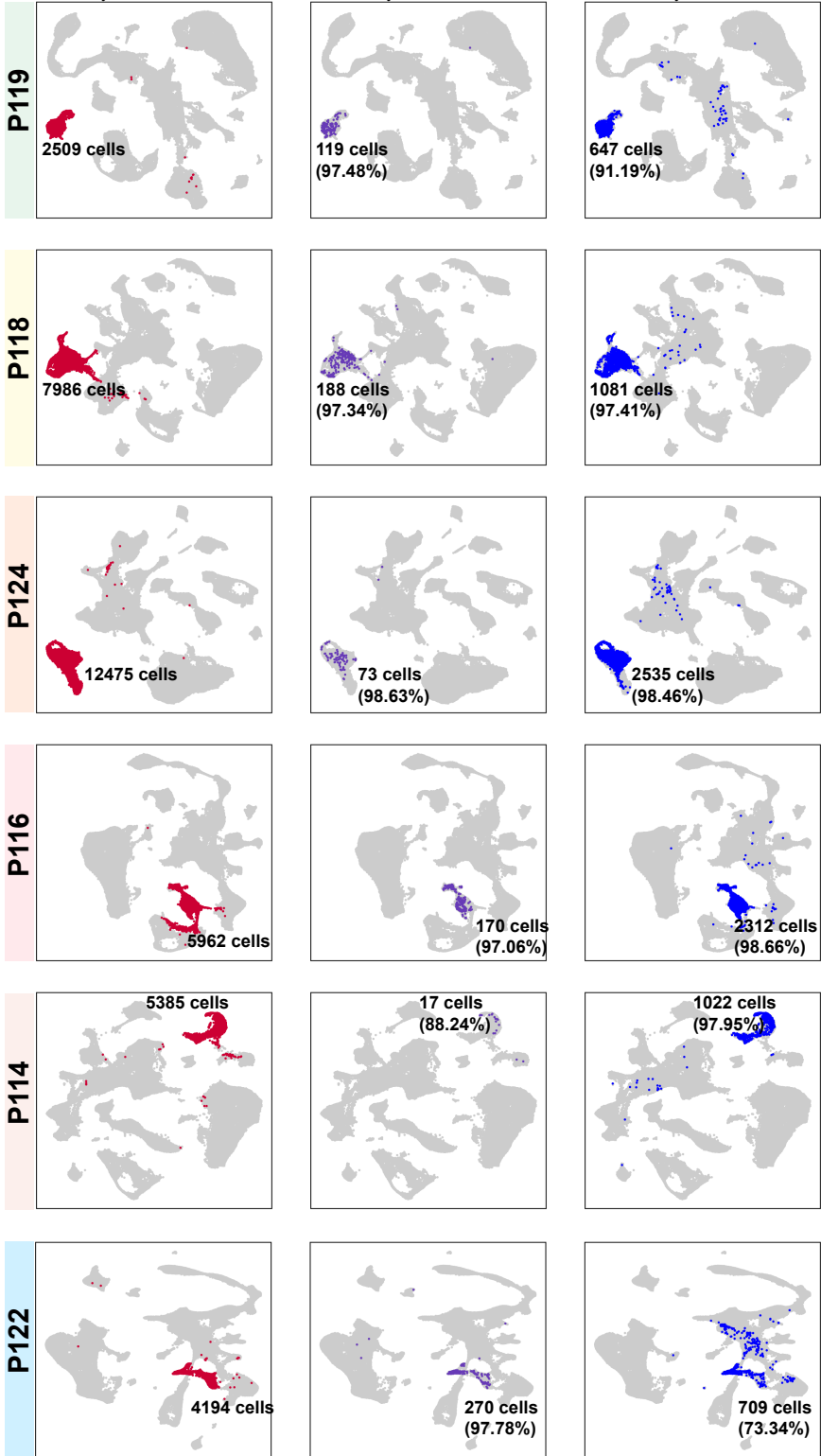
● yes ● no

mutation

● yes ● no

LAIP

● yes ● no

**Continued on next page**

**transcriptionally
predicted malignant cell**

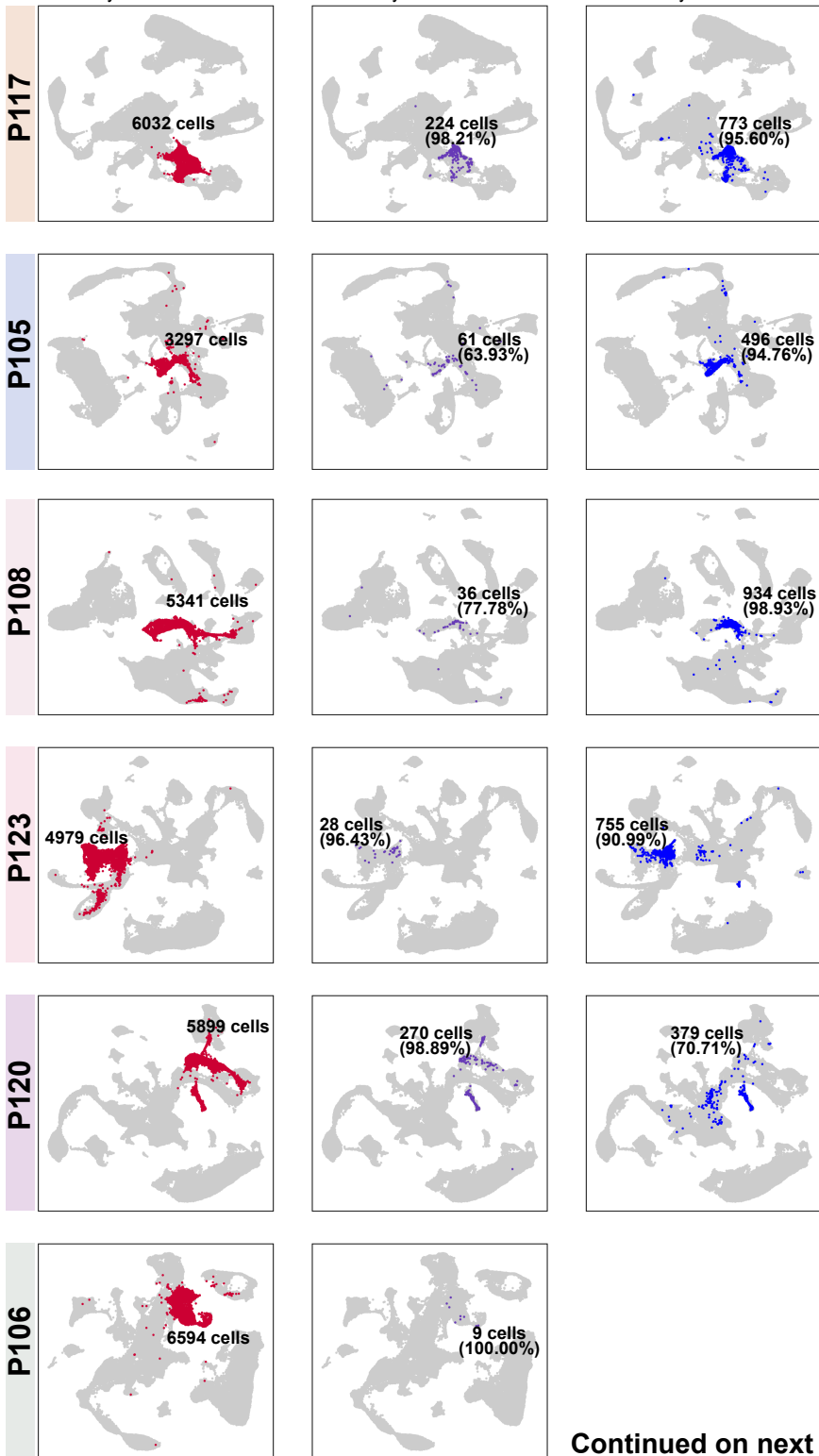
● yes ● no

mutation

● yes ● no

LAIP

● yes ● no



Continued on next page

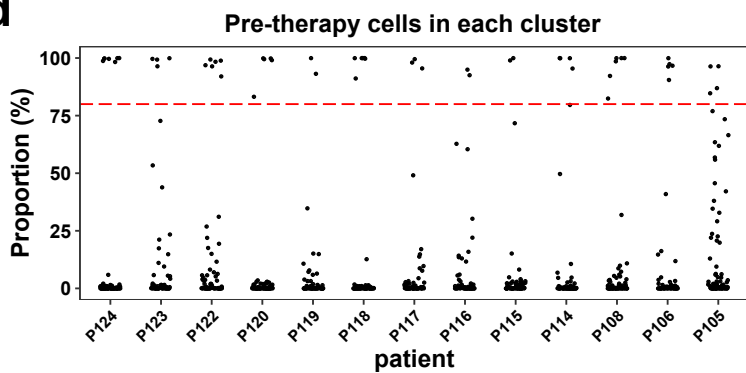
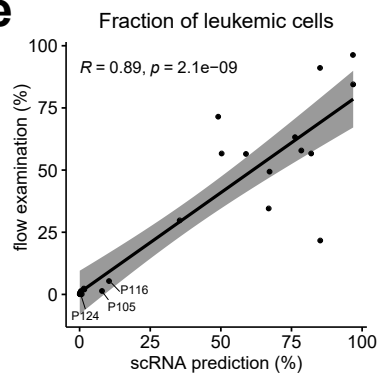
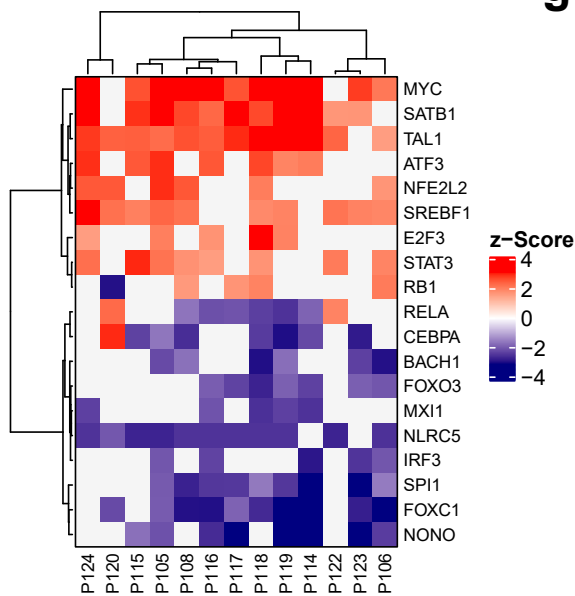
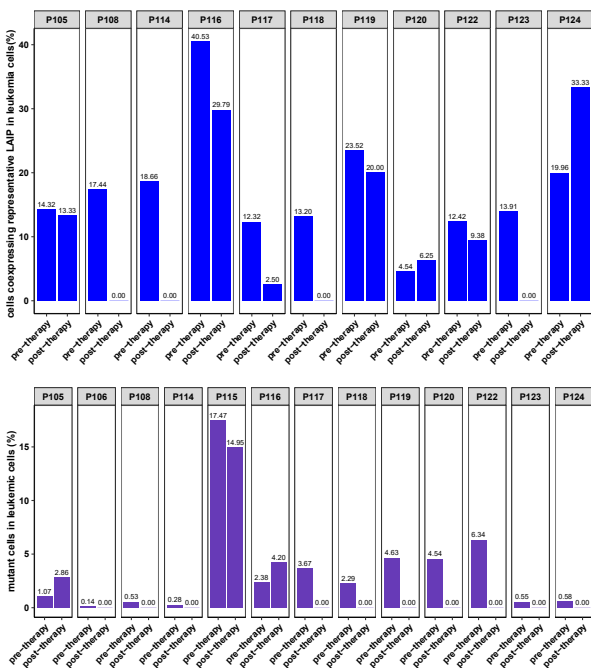
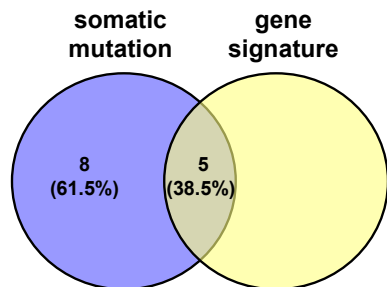
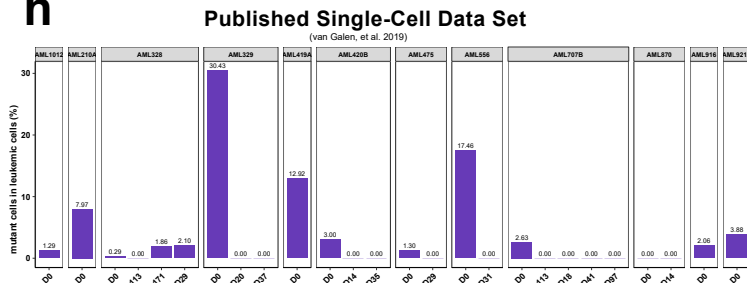
d**e****f****g****i****h**

Figure S2. Identification and validation of leukemic and normal cells in published and our scRNA-seq datasets

a UMAP visualization of the published healthy and AML scRNA-seq data. Cells are colored according to sample origins (left, malignant cells predicted by our approach are circled), genotypes at specific mutation sites (middle), or previous classifications using a machine learning classifier (right), as indicated at the top.

b Scatterplot comparing the fractions of leukemic cells predicted by our approach and previous classification shown in panel a. Each point corresponds to a sample.

c UMAP plots showing the clustering of paired pre- and post-therapy samples from each patient with healthy donors. Transcriptionally predicted leukemia cells (left), mutant cells (middle), and LAIP-coexpressing cells (right) are highlighted, respectively. The numbers of highlighted cells are shown. Of the highlighted cells, the percentage of cells transcriptionally predicted to be leukemic is shown in parentheses.

d Proportion of cells from the pre-therapy sample in each cell cluster for individual patients. A point represents a cluster. Clusters for each patient were defined by clustering scRNA-seq data shown in panel c and Fig.2b.

e Scatterplot comparing the proportions of leukemic cells predicted by flow examination and scRNA-seq. A point represents a sample. Post-therapy samples from P116, P105, and P124 are indicated.

f Heatmap displaying the upstream regulators enriched by highly expressed genes in leukemic cells compared to normal cells within each patient using IPA.

g Bar plots show the fractions of LAIP-coexpressing cells (top) and mutant cells (bottom) in the predicted leukemic cells in each sample shown in panel c. In the upper panel, only eleven patients with suitable LAIP markers are shown.

h Bar plots show the fraction of mutant cells in the predicted leukemic cells in each sample by our approach shown in panel a.

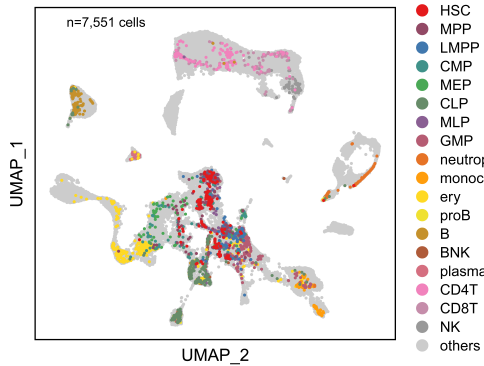
i Venn diagram shows the number and percentage of AML patients whose predicted leukemic cells were validated by independent methods.

R and p values in panels b and e were calculated using Pearson's correlation test.

Figure S3

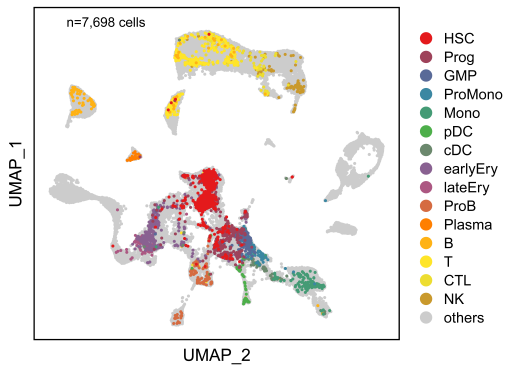
a Published FACS Sorted Single-Cell Data Set

(Xie X, et al., 2020)



Published Single-Cell Data Set

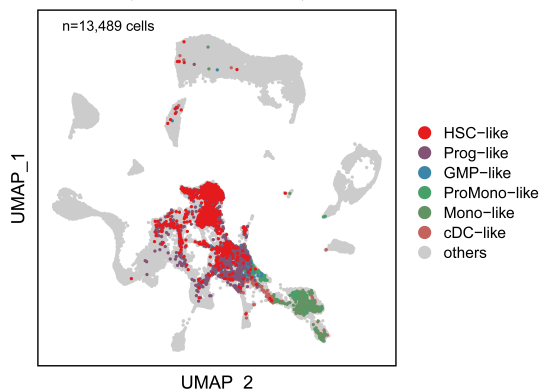
(van Galen P, et al., 2019)



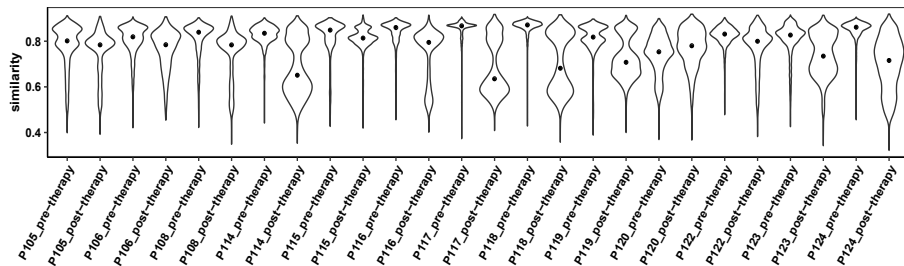
b

Published Single-Cell Data Set

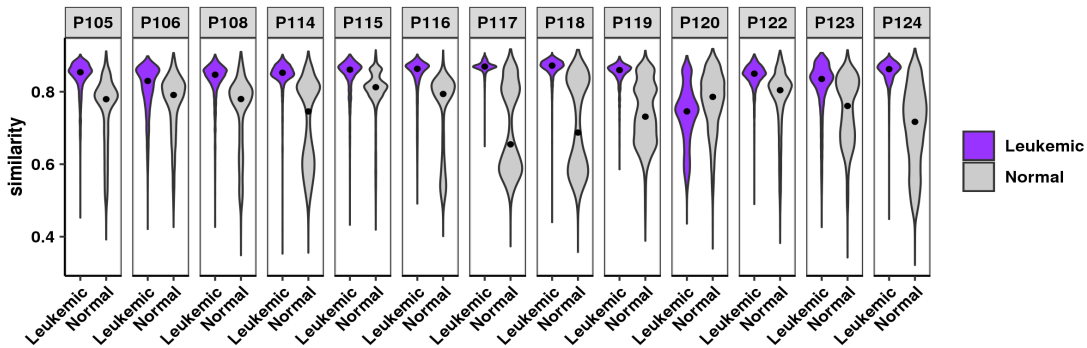
(van Galen P, et al., 2019)



c



d



Continued on next page

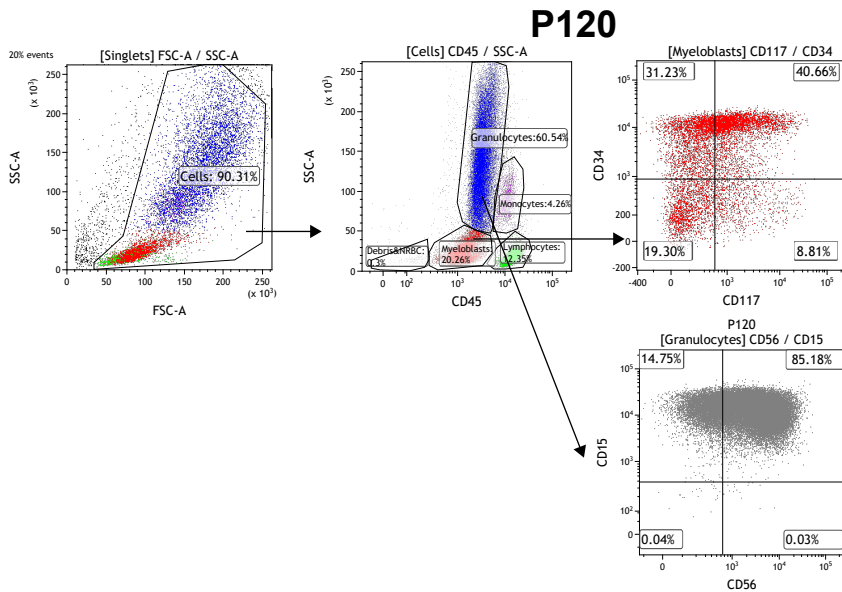
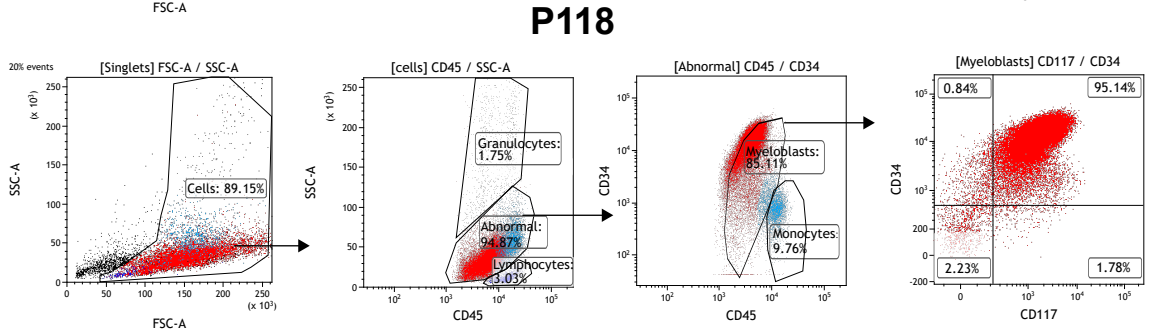
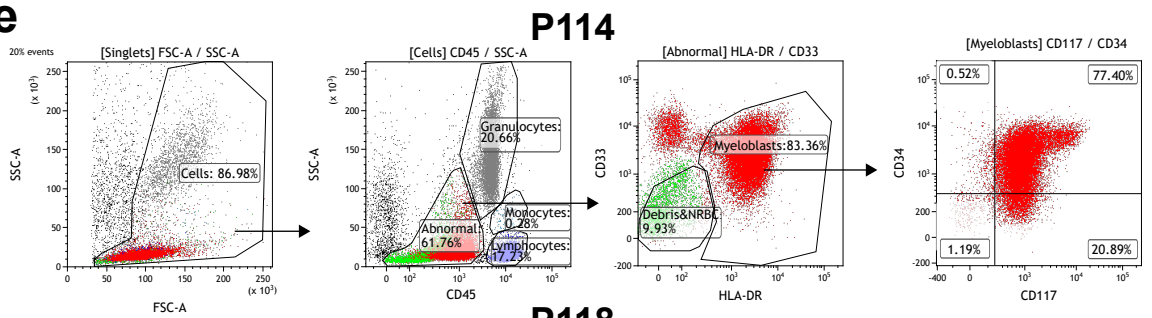
e

Figure S3. Cell type annotation of leukemia cells by projection onto the hematopoietic hierarchy

a, b UMAP plots display the projection of public flow cytometry-sorted healthy hematopoietic single-cell dataset (panel a, left), BMMC single-cell dataset (panel a, right), and malignant hematopoietic single-cell dataset (panel b) onto the hematopoietic hierarchy. Cells from each dataset are colored according to previously published classifications.

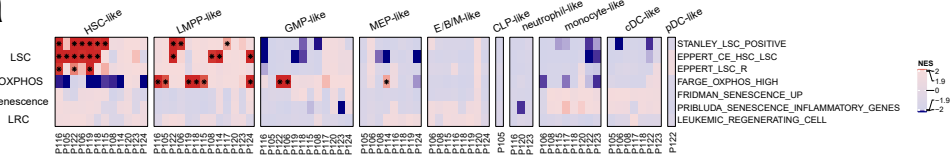
c Violin plots show the cosine similarity between cells and their nearest healthy neighbors in each sample.

d Violin plots show the cosine similarity between leukemia/normal cells and their nearest healthy neighbors in each patient.

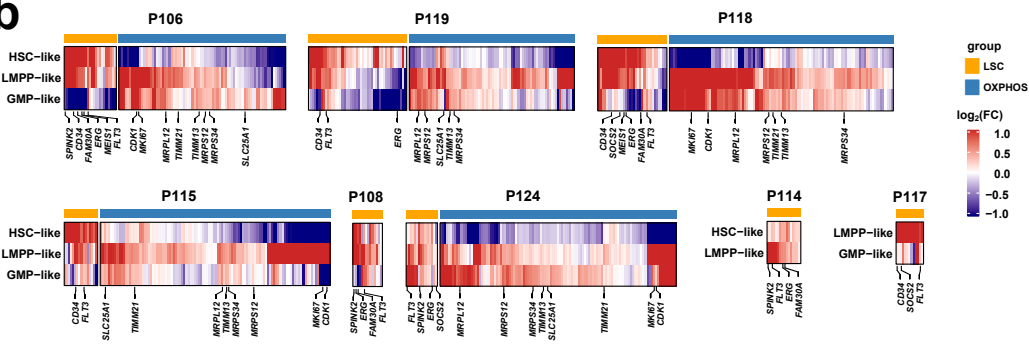
e Flow cytometry plots show the gating of pre-therapy bone marrow cells derived from AML patients (P114, P118, and P120) and their expression of stem and progenitor markers (CD34 and CD117).

Figure S4

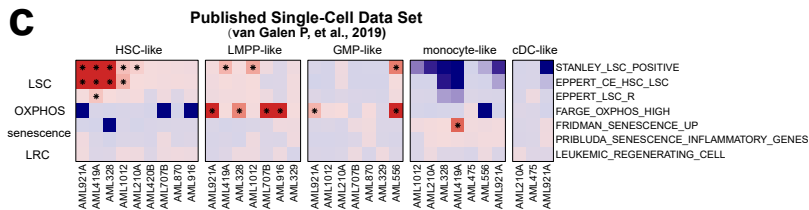
a



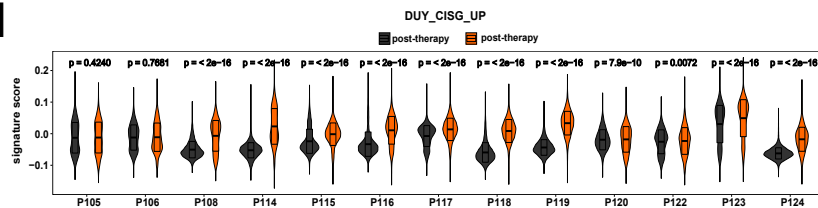
b



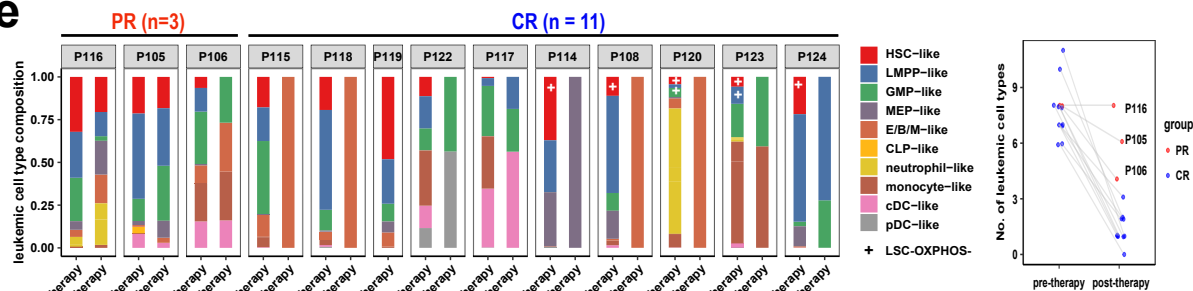
c



d



e



f

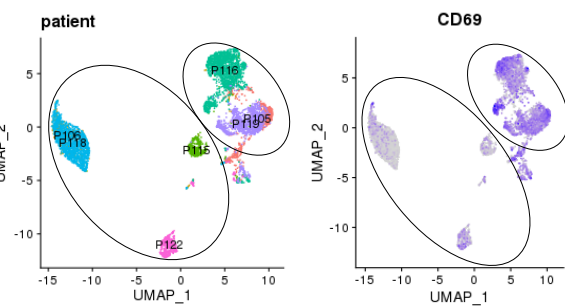


Figure S4. Expression signatures and dynamic changes of leukemic cell populations in our and published AML scRNA-seq datasets

a, c Heatmaps depicting the GSEA results of four known chemoresistance-related expression signatures (rows) for each leukemic population (columns) compared to all other leukemic populations within the same patient from our scRNA-seq dataset (panel a) and the published scRNA-seq dataset by van Galen, et al. 2019 (panel c). Colors indicate the normalized enrichment score (NES) values by GSEA analysis, and an asterisk signifies both $NES > 1.9$ and false discovery rate (FDR) < 0.001 .

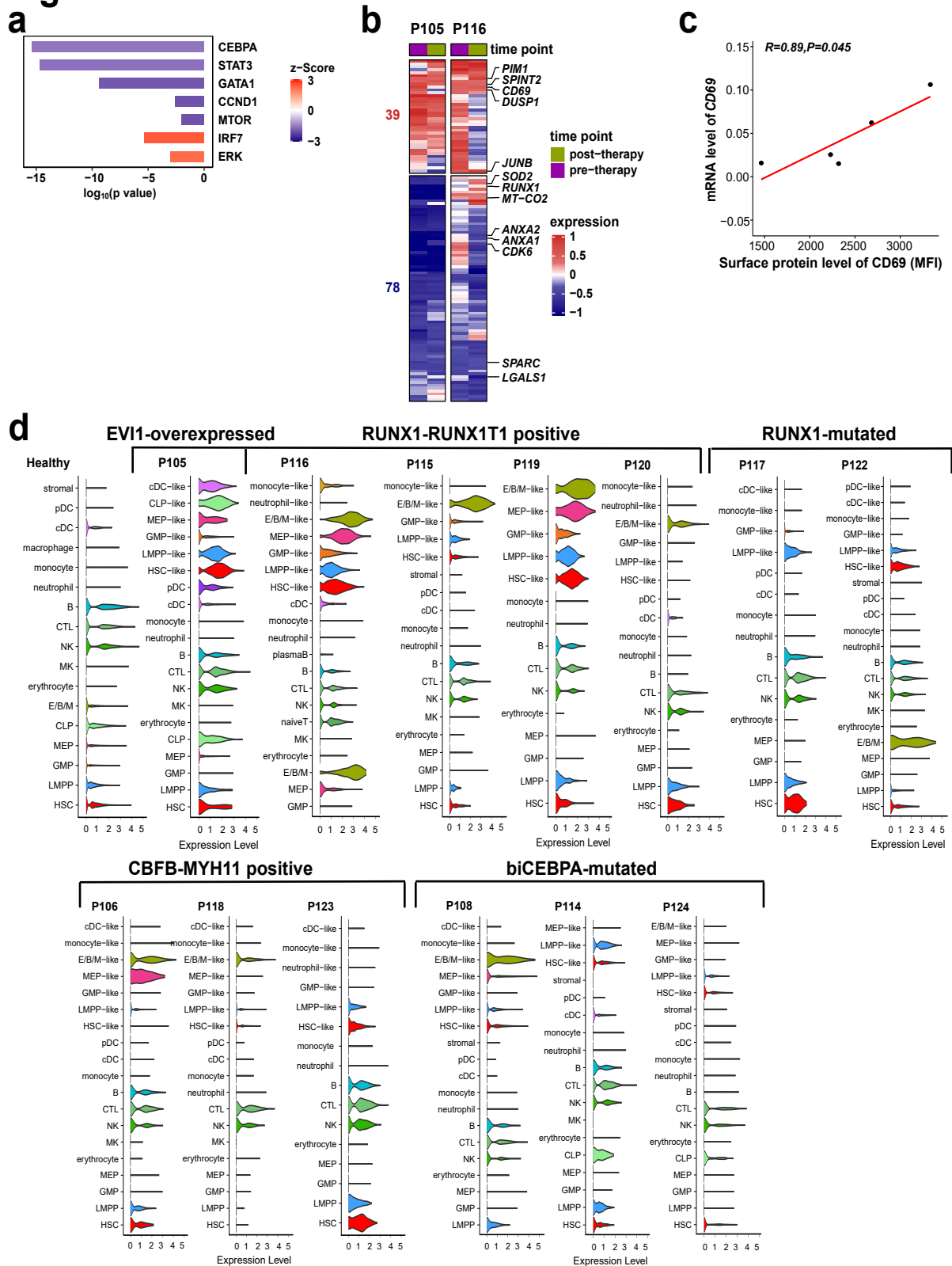
b Heatmaps showing expression fold changes (FC) of core enriched genes (columns) contributing to LSC and OXPHOS signatures in each HSPC-like population (rows) compared to all other leukemic populations within each patient. Core enriched genes are identified from GSEA results and those related to cell stemness and metabolism are indicated.

d Violin plot showing the signature scores of senescence in leukemic and normal cells resembling HSC, LMPP, GMP, monocyte, neutrophil, cDC, and pDC. P value for each patient was calculated between paired pre- and post-therapy samples using the Wilcoxon signed-rank test.

e (Left) Bar plot depicting the fractions of leukemic cell types in paired pre- and post-therapy samples from AML patients. A plus sign indicates the cell population that did not exhibit enrichment of LSC or OXPHOS signatures. (Right) Line plot showing the changes in leukemic cellular diversity. Three patients (P116, P105, and P106) who achieved partial remission (PR) are indicated.

f UMAP visualization of pre-therapy HSC-like leukemic cells from resistant patients (P116 and P105) and sensitive patients (P122, P106, P119, P118, and P115). Cells are colored by sample origin (left) and the expression level of *CD69* (right).

Figure S5



Continued on next page

e

Ng SW, et al., 2016

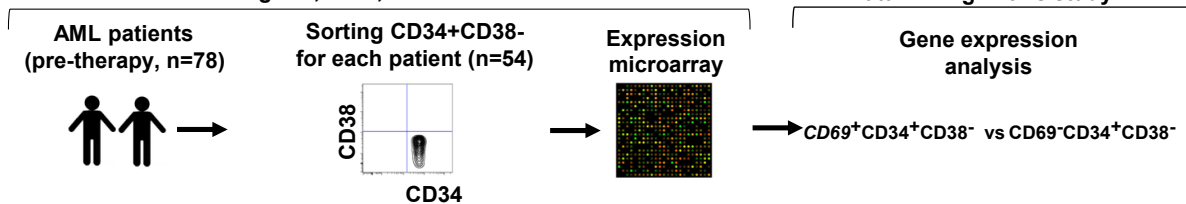
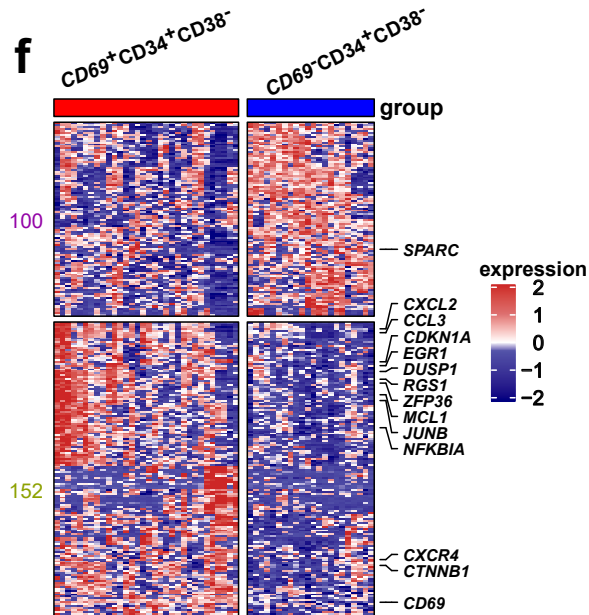
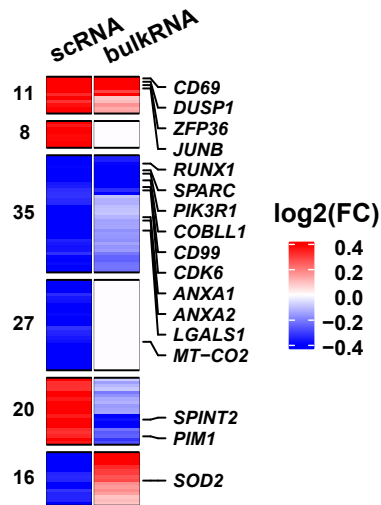
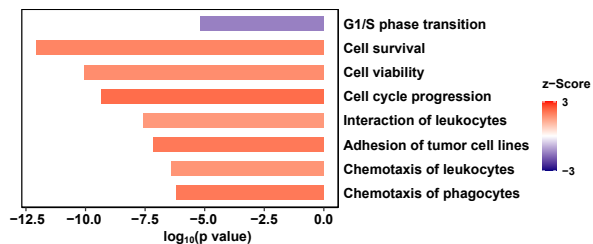
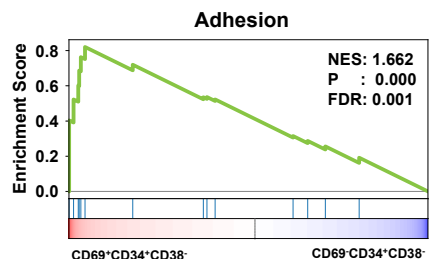
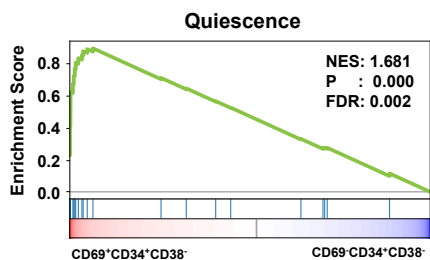
**f****g****h****i**

Figure S5. Gene expression profile of *CD69*⁺ HSC-like subpopulation

a Bar plot indicating representative upstream regulators predicted by the “scRNA DEGs” in Fig. 5a using IPA analysis.

b Heatmap showing the average expression levels of the “scRNA DEGs” (rows) in pre- and post-therapy HSC-like populations (columns) of resistant patients. The expression levels are normalized to those of sensitive patients.

c Correlation between mean fluorescence intensity (MFI) and mRNA expression of *CD69* in *CD34*⁺*CD38*⁻ HSC-like populations sorted from primary AML patients (n=5). R and P values were calculated using Pearson’s correlation test.

d Violin plots depicting the expression of *CD69* in different cell types from healthy donors and AML patients.

e Schematic diagram of bulk gene expression profiling and data analyses for AML patients performed by Ng SW, et al 2016 and this study. The sorted *CD34*⁺*CD38*⁻ cell populations were divided into *CD69*⁺*CD34*⁺*CD38*⁻ (n=32) and *CD69*⁻*CD34*⁺*CD38*⁻ (n=22) groups, based on the mean expression levels of *CD69*.

f Heatmap showing the relative expression of the DEGs between *CD69*⁺*CD34*⁺*CD38*⁻ and *CD69*⁻*CD34*⁺*CD38*⁻ groups (“bulkRNA DEGs”).

g Heatmap showing the expression fold changes of “scRNA DEGs” (rows) between the resistant and sensitive groups in Fig. 5a (the scRNA column) and those between *CD69*⁺*CD34*⁺*CD38*⁻ and *CD69*⁻*CD34*⁺*CD38*⁻ groups in panel e (the bulkRNA column). Red and blue indicate a gene with over 1.05-fold increase and decrease in expression, respectively.

h Bar plot showing representative biological processes predicted by the “bulkRNA DEGs” in panel f using IPA analysis.

i GSEA plots showing the enrichment of the quiescence (top) and adhesion (GO term: Positive regulation of leukocyte adhesion to vascular endothelial cells) (bottom) signatures in *CD69*⁺*CD34*⁺*CD38*⁻ cells compared to *CD69*⁻*CD34*⁺*CD38*⁻ cells.

DEGs related to adhesion/migration are indicated in panels b, f, and g.

Figure S6

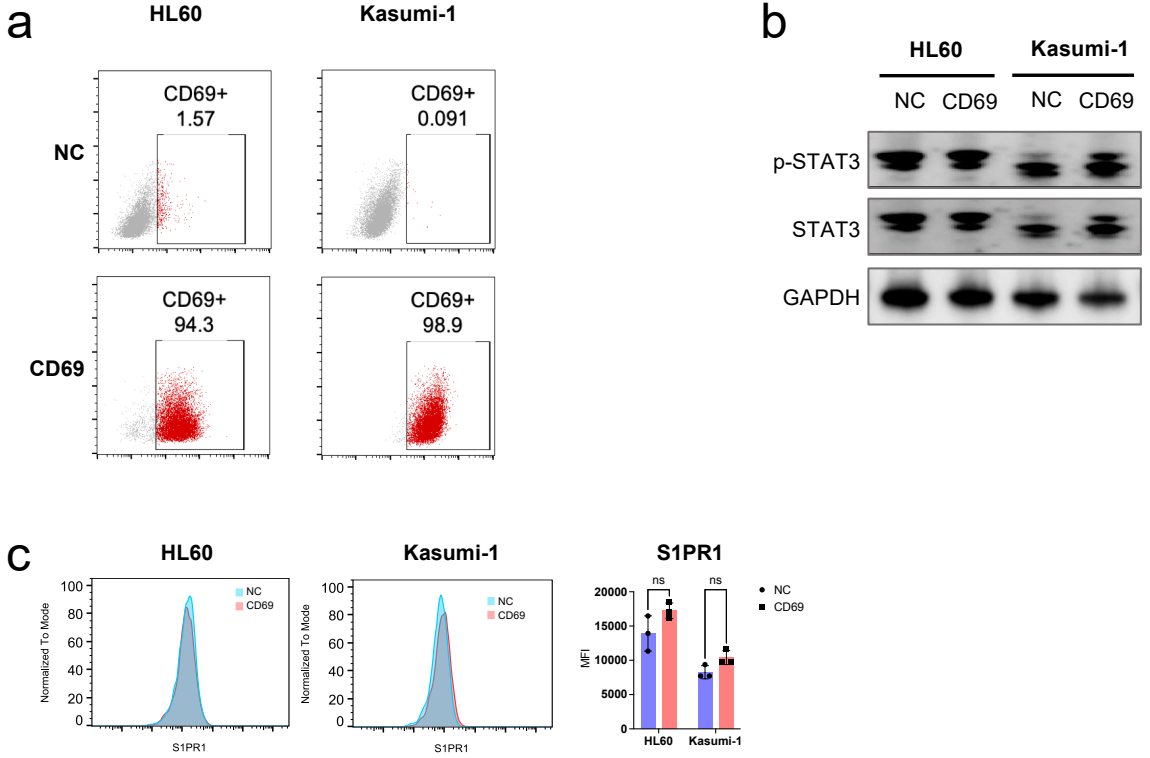


Figure S6. *CD69* overexpression did not affect the *STAT3* signaling pathway and *S1P1R* expression

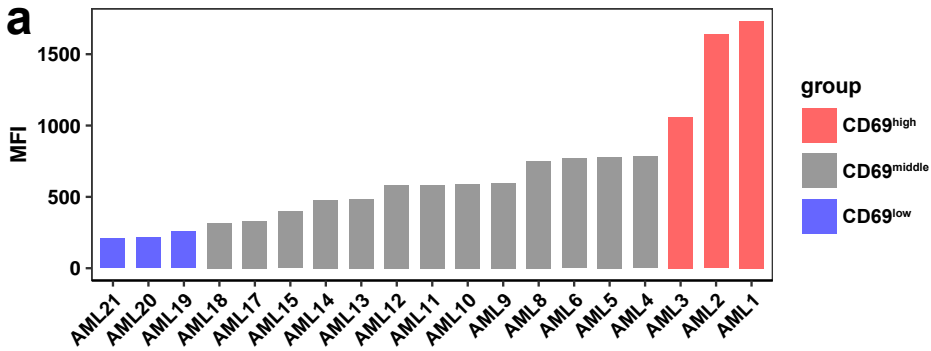
a Flow cytometry analyses of the cell surface protein *CD69* on negative control (NC) and *CD69*-overexpressing HL60 and Kasumi-1 cells. Percentages of *CD69*⁺ cells within total cells are indicated.

b Western blot showing the total and phosphorylated protein levels of *STAT3* in NC and *CD69*-overexpressing HL60 and Kasumi-1 cells.

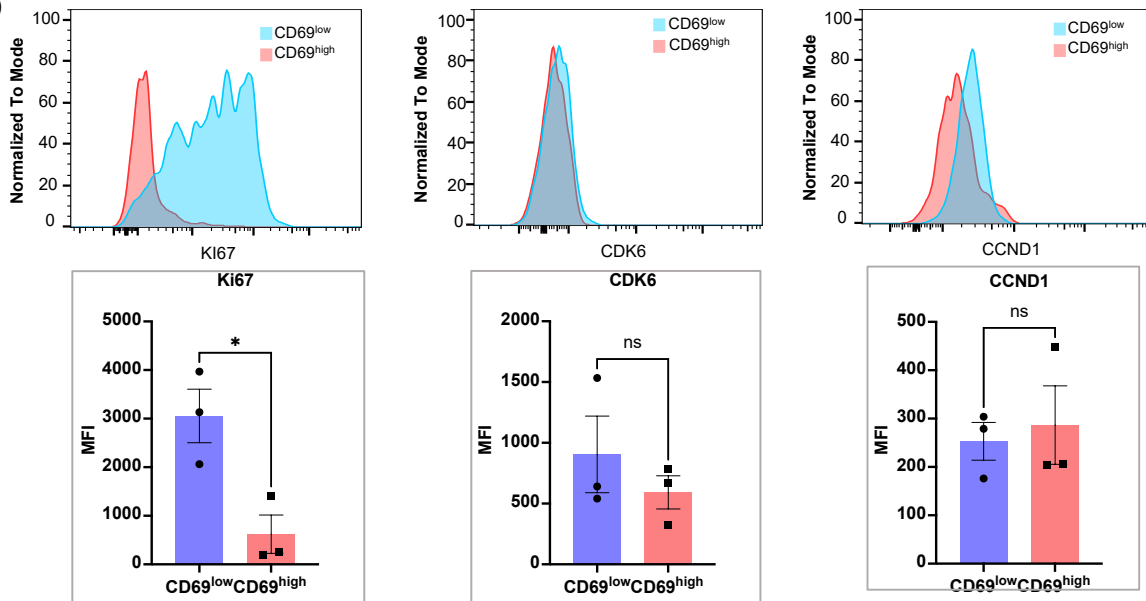
c Histogram (left) and statistical results (right) of flow cytometry analyses showing the cell surface protein levels of *S1P1R* on NC and *CD69*-overexpressing HL60 and Kasumi-1 cells. * $P < 0.05$; ** $P < 0.01$; *** $P < 0.001$; ns, not significant; t test. Mean \pm SEM values are shown.

Figure S7

a



b



c

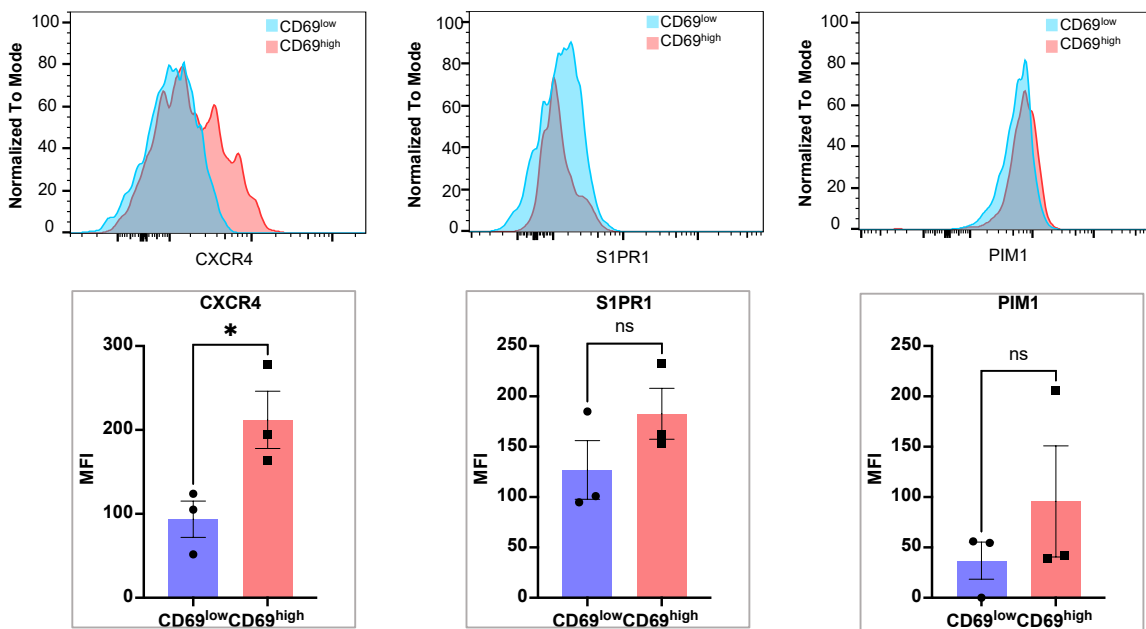


Figure S7. Suppression of cell proliferation markers and upregulation of adhesion chemokine receptors in CD69⁺CD34⁺CD38⁻ cells sorted from AML patients

a Histogram shows the surface protein levels of CD69 in CD34⁺CD38⁻ (HSC-like) cell populations sorted from pre-therapy BM samples of AML patients (n=19), ranked from lowest to highest. Cell populations with CD69 MFI ranking in the top 20% and bottom 20% were classified as the "CD69^{low}" group (n=3) and the "CD69^{high}" group (n=3), respectively. The remaining cell populations were classified as the "CD69^{middle}" group (n=13).

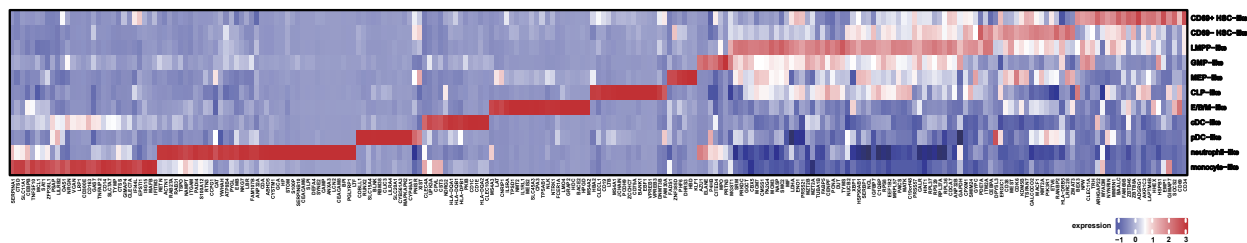
b Histogram (top) and statistical results (bottom) showing the protein levels of Ki67, CDK6, and CCND1 in the CD69^{high} and CD69^{low} groups in panel a.

c Histogram (top) and statistical results (bottom) showing the protein levels of CXCR4, PIM1, and S1PR1 in the CD69^{high} and CD69^{low} groups in panel a.

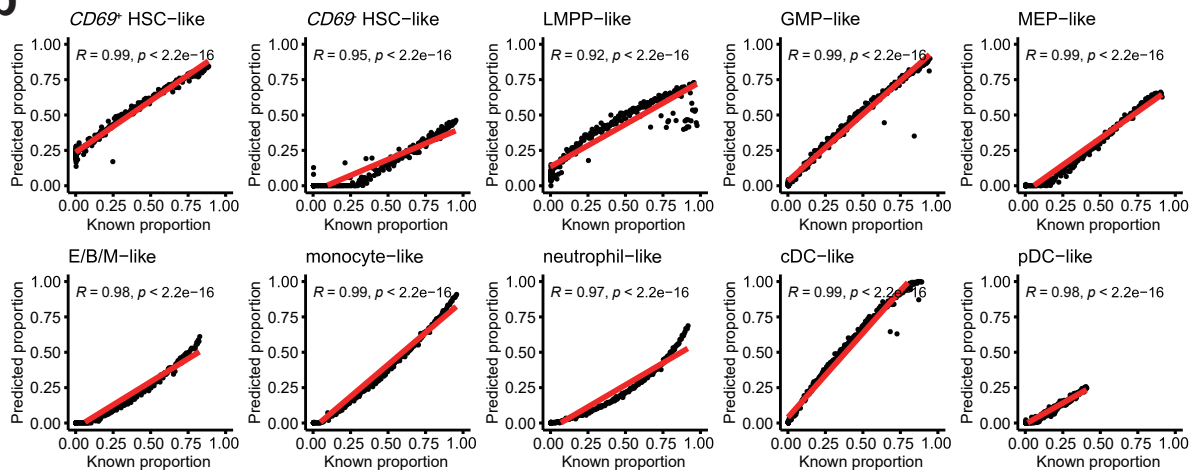
* P < 0.05; **P < 0.01; ***P < 0.001; ns, not significant; t test. Mean ± SEM values are shown for panels b-c.

Figure S8

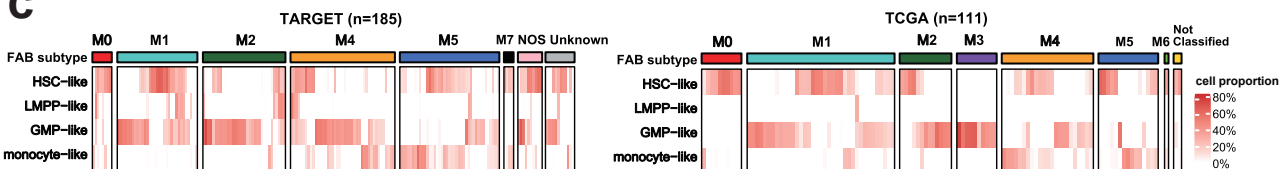
a



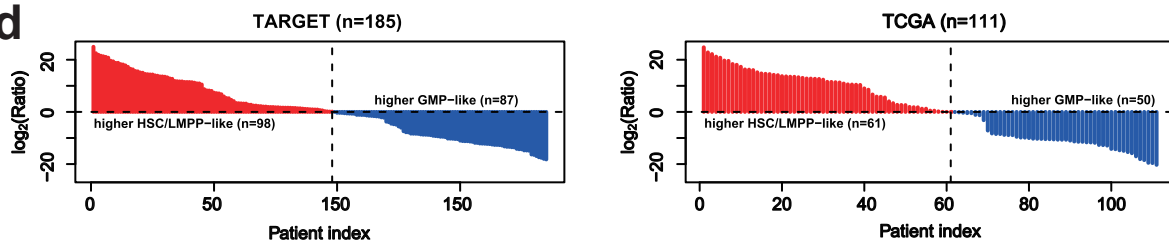
b



c



d



e

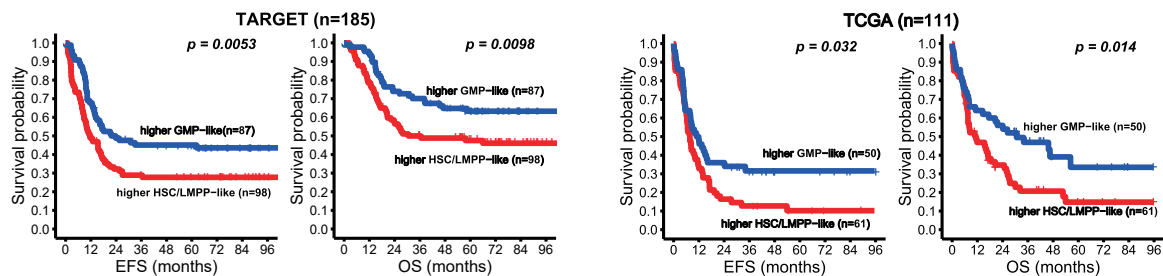


Figure S8. Estimation of cell type compositions using the EPIC deconvolution

a Heatmap representing differential average expression profiles of the 231-gene signature in 11 leukemic cell types.

b Scatterplots showing correlations between the inferred (y-axis) and known (x-axis) proportions of transcriptionally-defined leukemic cell types in simulation data generated from our scRNA-seq data. R and p values were calculated using Pearson's correlation test.

c Heatmaps showing the estimated proportions of leukemic cell types in pre-therapy samples of AML patients with different French–American–British (FAB) subtypes from public cohorts.

d The \log_2 -transformed ratio of estimated HSC/LMPP-like and GMP-like cell proportions within each AML patient in panel c. Patients are ranked by the ratios from highest to lowest and stratified into higher HSC/LMPP-like and higher GMP-like groups.

e Kaplan-Meier curves show the event-free survival (EFS) and overall survival (OS) of AML patients stratified by the ratios in panel d. Patients with higher HSC/LMPP-like proportions have worse outcomes compared to those with lower HSC/LMPP-like proportions. P-values were calculated using the log-rank test.

Figure S9

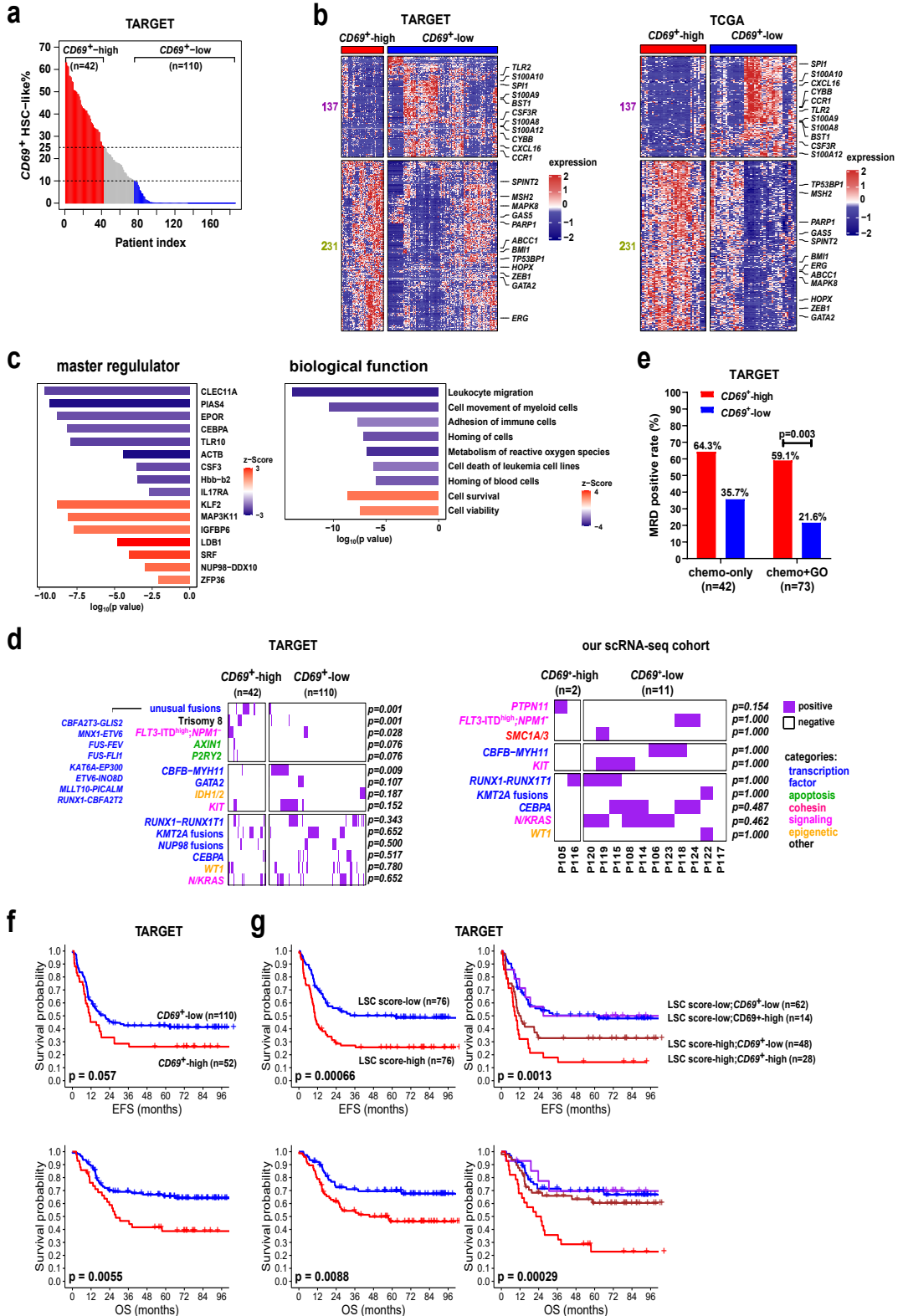


Figure S9. Gene expression profiles and clinical outcomes of AML patients with different *CD69*⁺ HSC-like cell proportions

a Estimated proportions of the *CD69*⁺ HSC-like subpopulation (*CD69*⁺ HSC-like%) in pre-therapy samples from TARGET-AML patients. Patients were grouped into *CD69*⁺-high (red), *CD69*⁺-middle (grey), and *CD69*⁺-low (blue) according to the *CD69*⁺ HSC-like%, with dashed black lines indicating the cutoffs.

b Heatmaps showing the relative expression of DEGs in pre-therapy samples between *CD69*⁺-high and *CD69*⁺-low patients in panel a. These DEGs exhibited consistent expression differences between the TARGET and TCGA cohorts. Some representative genes are indicated.

c Representative master regulators and biological functions with dysregulated transcription activities predicted by the DEGs in panel b using IPA analysis.

d Heatmaps showing the presence of genomic alterations in pre-therapy samples from TARGET-AML patients and our scRNA-seq cohort. Genomic alterations (row) are colored according to the biological functions of their corresponding genes. The cohesin term includes mutations of the core complex subunits *STAG2*, *RAD21*, *SMC1A/3/5*, or its modulator *PDS5B*. *FLT3*-ITD^{high}; *NPM1*⁻ represents wild type *NPM1* with *FLT3*-internal tandem duplication (ITD) with a high allelic ratio (≥ 0.5). Unusual fusions are indicated.

e Flow cytometry-based measurable residual disease (MRD) positive rates in TARGET-AML patients at the end of the first cycle of chemotherapy regimen. Patients were defined as MRD-positive with the clinical cutoff of 0.1% at the end of the first cycle of induction therapy. Chemo-only and chemo+GO represent patients who received standard chemotherapy without or with gemtuzumab ozogamicin (GO), respectively.

f Kaplan-Meier curves showing the survival of TARGET-AML patients stratified by *CD69*⁺ HSC-like% in panel a.

g Kaplan-Meier curves showing the survival of TARGET-AML patients stratified by LSC score alone or combined with *CD69*⁺ HSC-like% in panel a.

All p values in panel d were calculated using Fisher's test.

All p values in panels e, f and g were calculated using the log-rank test.